Measurement of the $\Xi^0 \rightarrow \Sigma^0\gamma$ Branching Ratio and Asymmetry Parameter

S. Teige, A. Beretvas,[a] A. Caracappa,[b] T. Devlin,[c] H. T. Diehl, K. Krueger,[d] and G. B. Thomson
Department of Physics and Astronomy, Rutgers—The State University of New Jersey, Piscataway, New Jersey 08854

P. Border,[e] P. M. Ho, and M. J. Longo
Department of Physics, University of Michigan, Ann Arbor, Michigan 48109

J. Duryea, N. Grossman, K. Heller, M. Shupe,[f] and K. Thorne[a]
School of Physics and Astronomy, University of Minnesota, Minneapolis, Minnesota 55455
(Received 15 May 1989)

From 85 ± 10 examples of the decay $\Xi^0 \rightarrow \Sigma^0\gamma$ we have measured the decay branching ratio $\Gamma(\Xi^0 \rightarrow \Sigma^0\gamma)/\Gamma(\Xi^0 \rightarrow \Lambda\pi^0) = [3.56 \pm 0.42(\text{stat}) \pm 0.10(\text{syst})] \times 10^{-3}$ and the asymmetry parameter $\alpha(\Xi^0 \rightarrow \Sigma^0\gamma) = 0.20 \pm 0.32(\text{stat}) \pm 0.05(\text{syst})$.

PACS numbers: 13.40.Hq, 14.20.Jn

In an experiment performed at Fermilab we have observed for the first time the weak-radiative decay $\Xi^0 \rightarrow \Sigma^0\gamma$. Such weak-radiative decays are an excellent laboratory to study the strong interaction as it modifies the well understood electroweak interaction.[1] Previously, only observations of $\Lambda \rightarrow n\gamma$,[2] $\Sigma^+ \rightarrow p\gamma$,[3] and $\Xi^- \rightarrow \Sigma^-\gamma$ (Ref. 4) had been published. Several theoretical attempts to calculate the rates[5-10] and decay asymmetries[5,7-10] of hyperon radiative decays have been published; predictions for Ξ^0 decay are summarized in Table I. Predictions for the branching ratio for $\Xi^0 \rightarrow \Sigma^0\gamma$ range over almost 2 orders of magnitude. Previously, an upper limit of 8×10^{-3} for $\Gamma(\Xi^0 \rightarrow \Sigma^0\gamma)/\Gamma(\Xi^0 \rightarrow \Lambda\pi^0)$ has been published.[11] An accurate measurement of the parameters for $\Xi^0 \rightarrow \Sigma^0\gamma$ will help to constrain further the theoretical calculations and give insight into the effects complicating them.

The decay $\Xi^0 \rightarrow \Sigma^0\gamma$, $\Sigma^0 \rightarrow \Lambda\gamma$, $\Lambda \rightarrow p\pi^-$ has a topology identical to $\Xi^0 \rightarrow \Lambda\pi^0$, $\pi^0 \rightarrow \gamma\gamma$, $\Lambda \rightarrow p\pi^-$, and our apparatus was equally sensitive to both decay chains; in a ratio measurement such as ours, many systematic effects can be expected to cancel. These two processes are kinematically ambiguous over two-thirds of the available phase space due to the finite resolution of our apparatus.

TABLE I. A summary of theoretical predictions for $\Xi^0 \rightarrow \Sigma^0\gamma$.

$10^3 \times$(Branching ratio)	Asymmetry	Reference
10	−0.9	5
9.1	···	6
7.2	−0.96	8
5.87	−0.58	7
2.62–4.58	0.81–0.97	10
1.48	−0.30	9
0.23	−0.99	9

A neutral beam was made by 800-GeV/c protons striking a 9.6-cm-long tungsten target. The charged secondary particles were swept out of the beam by a 27-Tm sweeper magnet. Neutral secondaries, including Ξ^0's, passed through a collimator with a 3.2-mm-diam defining aperture located in the magnet 4.0 m from the target. The detector[12] (Fig. 1) consisted of three 2-mm wire-spacing multiwire proportional chamber (MWPC's), followed by an analysis magnet with a 1.6-GeV/c transverse-momentum bend, followed by three more MWPC's. These chambers were used to reconstruct the vector momenta of charged tracks.

Two 1-mm-thick scintillation counters, $V1$ and $S1$ separated by 18.6 m, defined the decay region by indicating a neutral particle entering and its charged decay products leaving. Two scintillator hodoscopes, A and B, were used to trigger on events with a pair of oppositely charged tracks. An additional scintillation counter, $P1$ or $P2$ (depending on analysis magnet polarity), covered the region illuminated by the protons from $\Lambda \rightarrow p\pi^-$.

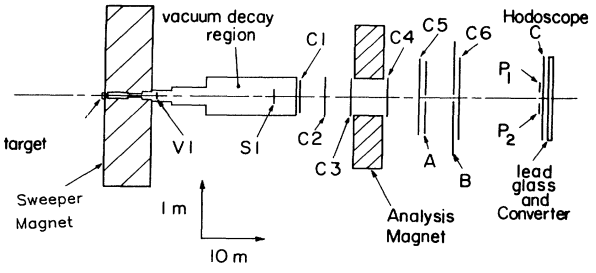

FIG. 1. Plan view of the apparatus showing the 800-GeV/c proton beam, the target, sweeper magnet, scintillation counters $V1$ and $S1$, multiwire proportional chambers $C1$–$C6$, the A–C scintillator hodoscopes, and the lead-glass array.

These requirements selected $\Lambda \rightarrow p\pi^-$ decays. Downstream of the last MWPC was a 3-radiation-length ($3L_{\text{rad}}$) lead converter followed by an array of 86 $10\times10\times40$-cm^3 ($12L_{\text{rad}}$ deep) lead-glass blocks. The center block of the array was missing to allow the neutral beam to pass through. The trigger required two or more separated clusters of blocks, not associated with charged tracks as determined by hodoscope C, to have a signal above a threshold of 2 GeV. This selected events with more than one photon.

When the trigger requirements were satisfied, MWPC hits, digitized pulse heights and times from the lead glass, and scintillator latches were recorded. A total of 8×10^6 triggers were taken. Off line the charged tracks were reconstructed and events with a Λ were selected by the following requirements: (1) There were exactly two charged tracks of opposite sign intersecting in the decay region, and (2) the effective mass of the track pair, under the hypothesis they were $p^+\pi^-$, was within 10 MeV/c^2 of the Λ mass. The Λ momentum vector was then determined by a kinematic fit constrained by the Λ mass. Further requirements which selected both $\Xi^0 \rightarrow \Sigma^0\gamma$ and $\Xi^0 \rightarrow \Lambda\pi^0$ candidates were as follows: (3) There were exactly two clusters of hits in the lead-glass array not associated with charged tracks, and (4) each cluster had an energy larger than 5.6 GeV. To complete the reconstruction of the event, the photon momentum vectors were determined from the energy and location of the clusters in the lead glass and the Ξ^0 decay vertex. The Ξ^0 vertex was chosen along the reconstructed path of the Λ such that the $\Lambda\gamma\gamma$ effective mass was identically equal to the Ξ^0 mass. If this vertex was, within our resolution of typically 0.5 m, upstream of the Λ vertex, the event passed initial reconstruction requirements.

Additional cuts were imposed to reduce the background due to beam Λ's with uncorrelated photons and to isolate Ξ^0's in the beam phase space. The photon arrival times were required to be coincident with the trigger. The Λ was projected to the target and the transverse distance to the target axis was required to be larger than 0.4 cm. It was required that the angle $|\delta|$ between the reconstructed Ξ^0 momentum and the vector from the target to the Ξ^0 decay vertex be less than 1 mrad. The Ξ^0 was projected to the target plane and required to be within 0.6 cm of the target center. The Ξ^0 direction was required to be within 1.5σ of the average beam direction. To eliminate the effects of the uninstrumented beam hole in the lead glass, events with a photon cluster with its maximum energy block adjacent to the hole were eliminated. Applying these selection criteria produced a data sample of 71 832 Ξ^0 decays. Table II summarizes the effects of the cuts on the data sample.

To select $\Xi^0 \rightarrow \Sigma^0\gamma$ events we required $|m_{\gamma\gamma} - m_{\pi^0}| > 40$ MeV/c^2. Monte Carlo calculations indicate this cut rejected more than 99% of the $\Xi^0 \rightarrow \Lambda\pi^0$ events while passing 35.7% of the $\Xi^0 \rightarrow \Sigma^0\gamma$ events. The Σ^0 peak was visible in the $\Lambda\gamma$ effective-mass distribution after this cut (Fig. 2). The final answer was stable against variations of the value of this cut.

TABLE II. Event selection.

Cut	Events
Trigger	8×10^6
Initial reconstruction	330 427
$\|\delta\|$ cut	272 347
Cluster timing cut	232 236
Reconstructed Ξ^0 points to target	205 490
Λ to target distance	161 887
Ξ^0 direction within 1.5σ	113 009
No hole clusters	71 832
$\|m_{\gamma\gamma} - m_{\pi}\|$	240

Monte Carlo samples reproduced all the data distributions we examined including the $\gamma\gamma$ effective mass, the beam phase space, hit distributions in the chambers and hodoscopes, and block multiplicity in the photon clusters. Figure 3 compares the $\gamma\gamma$ effective mass from Monte Carlo $\Xi^0 \rightarrow \Lambda\pi^0$ events to $\Xi^0 \rightarrow \Lambda\pi^0$ events from the data.

To extract the branching ratio, the $\Lambda\gamma$ effective-mass distribution was fitted to a sum of the Monte Carlo $\Lambda\gamma$ effective-mass distribution for $\Xi^0 \rightarrow \Sigma^0\gamma$ and a constant background. Both $\Lambda\gamma$ combinations were used since both

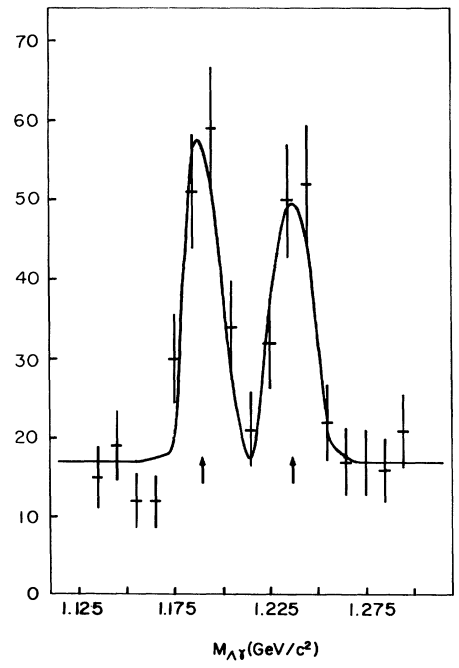

FIG. 2. The $\Lambda\gamma$ effective-mass distribution. Both combinations of $\Lambda\gamma$ effective mass are plotted. The arrows show the location of the Σ^0 mass (1.192 GeV/c^2) and its reflection. The curve is the result of a fit described in the text.

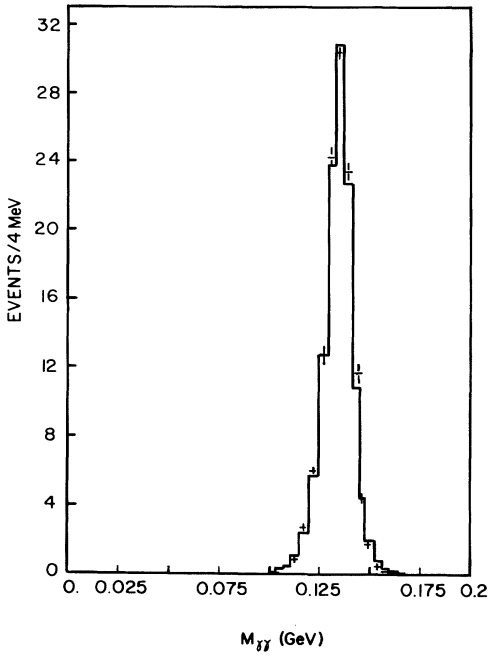

FIG. 3. The $\gamma\gamma$ effective mass for the data (solid line) and Monte Carlo events (crosses).

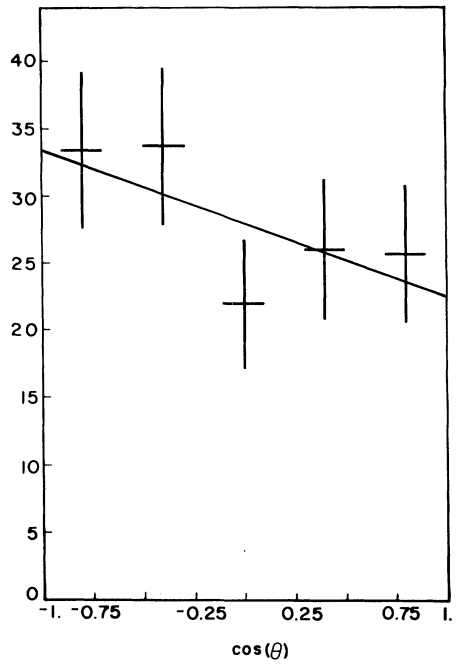

FIG. 4. The distribution of $\cos\theta$ used to extract the asymmetry parameter. The straight line is the result of the fit.

had narrow distributions for $\Xi^0 \to \Sigma^0\gamma$ events. The fit, shown as the smooth curve in Fig. 2, yielded 85 ± 10 $\Xi^0 \to \Sigma^0\gamma$ events over a background of 70 events within 15 MeV/c^2 of the Σ^0 mass and had $\chi^2/\mathrm{DF} = 0.9$.

The branching ratio could be calculated once the relative acceptance for the two decay modes was known. The Monte Carlo $\Xi^0 \to \Sigma^0\gamma$ and $\Xi^0 \to \Lambda\pi^0$ samples were subjected to the same analysis programs that extracted the data distributions. The overall acceptance for the $\Xi^0 \to \Lambda\pi^0$ mode was 1.07 ± 0.02 times the acceptance for the $\Xi^0 \to \Sigma^0\gamma$ mode. The $\gamma\gamma$ effective-mass cut applied to the $\Xi^0 \to \Sigma^0\gamma$ sample kept 35.7% of the sample and yielded an overall acceptance correction of 3.00 ± 0.06. The result was

$$\frac{\Gamma(\Xi^0 \to \Sigma\gamma)}{\Gamma(\Xi^0 \to \Lambda\pi)} = \frac{(85 \pm 10)/0.357}{71832 - 238} \times 1.07 = [3.56 \pm 0.42(\mathrm{stat})] \times 10^{-3}. \quad (1)$$

The denominator is the number of events passing all cuts except the 40-MeV/c^2 $\gamma\gamma$ effective-mass cut minus the total number of $\Xi^0 \to \Sigma^0\gamma$ events corrected for acceptance. Based on Fig. 2 we estimate the background in the denominator to be $< 1\%$ and we neglect it. Variation of the value of the $\gamma\gamma$ effective-mass cut leads to a 2% variation on the branching-ratio result. These effects, along with the 2% uncertainty in the ratio of acceptances, added in quadrature yield a systematic uncertainty of ± 0.10.

To calculate the asymmetry parameter, all events within ± 15 MeV/c^2 of the Σ^0 mass were selected and the angle θ between the proton and the boost axis of the Σ^0 in the rest frame of the Λ calculated. One expects a distribution of the form

$$\frac{dN}{d(\cos\theta)} = N_0(1 - \alpha_\Lambda \alpha_\Xi \cos\theta), \quad (2)$$

where α_Λ was taken to be 0.642 ± 0.013 [13] and the desired asymmetry parameter is α_Ξ. To determine how the background affects this distribution, events in the final sample but outside the 15-MeV/c^2 mass cut were examined. For these background events the smallest $\Lambda\gamma$ mass combination was selected corresponding to the choice made for the data events. The effect of the background on the signal was estimated by fitting the background to a distribution

$$\frac{dN}{d(\cos\theta)} = B(1 + \alpha_B \cos\theta), \quad (3)$$

where B is the number of background events and $\alpha_B = -0.33 \pm 0.17$ from the fit. It was assumed that this distribution in $\cos\theta$ also characterized the background under the Σ^0 mass peak. The background-subtracted distribution in $\cos\theta$ was corrected for acceptance by

Monte Carlo calculation and fitted by Eq. (2). The asymmetry parameter α_Ξ was found to be $0.20 \pm 0.32(\text{stat})$. The quoted error includes the effect of the statistical uncertainty in the parametrization of the background. Figure 4 shows the distribution and the result of the fit. Systematic errors were investigated by recalculating α_B from events where the photons from one event were substituted for the photons from another. These artificial events simulated the background under the mass peak due to events with uncorrelated photons. Differences in these measurements of α_B contributed a systematic error of ± 0.05 to the measurement of α_Ξ.

In conclusion, we have observed 85 ± 10 $\Xi^0 \to \Sigma^0\gamma$ events in a sample of 71 832 Ξ^0 decays. When corrected for acceptance this yields a branching ratio

$$\frac{\Gamma(\Xi^0 \to \Sigma^0\gamma)}{\Gamma(\Xi^0 \to \Lambda\pi^0)} = [3.56 \pm 0.42(\text{stat}) \pm 0.10(\text{syst})] \times 10^{-3}.$$

The asymmetry parameter was measured to be

$$\alpha_\Xi = 0.20 \pm 0.32(\text{stat}) \pm 0.05(\text{syst}).$$

Our branching-ratio result disagrees at the 3σ level with all predictions listed in Table I except those of Ref. 10 though the prediction of Ref. 10 appears to conflict with the asymmetry parameter measurement.

We wish to thank L. Pondrom for the loan of the MWPC system and the staffs of the Fermilab Experimental Areas and Computing departments for their assistance. This work was supported by the National Science Foundation and the Department of Energy.

[a]Present address: Fermi National Accelerator Laboratory, P.O. Box 500, Batavia, IL 60510.

[b]Present address: National Synchrotron Light Source, Brookhaven National Laboratory, Upton, NY 11973.

[c]On leave 1988–1990; present address: Fermi National Accelerator Laboratory, P.O. Box 500, Batavia, IL 60510.

[d]Present address: Division of Natural Sciences and Mathematics, Northeastern State University, Tahlequah, OK 74464.

[e]Present address: School of Physics and Astronomy, University of Minnesota, Minneapolis, MN 55455.

[f]Present address: Department of Physics, University of Arizona, Tucson, AZ 85721.

[1]Mary K. Gaillard *et al.*, Phys. Lett. **158B**, 158 (1985).

[2]S. F. Biagi *et al.*, Z. Phys. C **30**, 201 (1986).

[3]S. F. Biagi *et al.*, Z. Phys. C **28**, 495 (1985); M. Kobayashi *et al.*, Phys. Rev. Lett. **59**, 868 (1987).

[4]S. F. Biagi *et al.*, Z. Phys. C **35**, 143 (1987).

[5]M. Scadron and L. Thebaud, Phys. Rev. D **8**, 2190 (1973).

[6]F. J. Gilman and A. B. Wise, Phys. Rev. D **19**, 976 (1979).

[7]K. G. Rauh, Z. Phys. C **10**, 81 (1981).

[8]M. B. Gavela *et al.*, Phys. Lett. **101B**, 417 (1981).

[9]A. N. Kamal and R. C. Verma, Phys. Rev. D **26**, 190 (1982).

[10]R. C. Verma and Avinash Sharma, Phys. Rev. D **38**, 1443 (1988).

[11]J. R. Bensinger *et al.*, Phys. Lett. B **215**, 195 (1988).

[12]N. Grossman *et al.*, Phys. Rev. Lett. **59**, 18 (1987); P. Border, Ph.D. thesis, University of Michigan, 1988 (unpublished).

[13]O. E. Overseth and R. F. Roth, Phys. Rev. Lett. **19**, 391 (1967); W. E. Cleland *et al.*, Nucl. Phys. **B40**, 221 (1972).